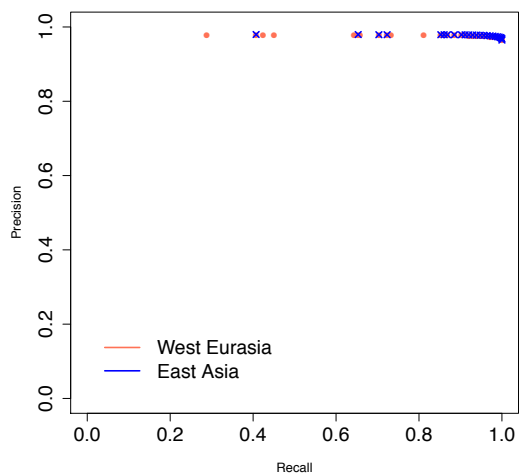


Current Biology, Volume 26

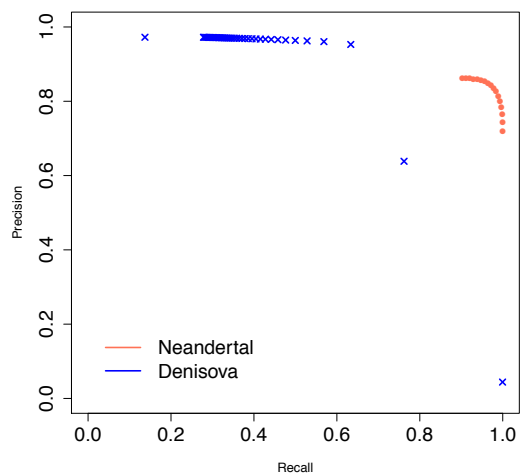
Supplemental Information

**The Combined Landscape of Denisovan
and Neanderthal Ancestry in Present-Day Humans**

Sriram Sankararaman, Swapan Mallick, Nick Patterson, and David Reich



(a)



(b)

Figure S1: Empirical precision-recall curves for archaic local ancestry inference (related to main text Experimental Procedures). (a) Empirical precision-recall curve of the modified method for inferring Neanderthal local ancestry in West Eurasian and East Asian populations. (b) Empirical precision-recall curve of the modified method for inferring Neanderthal and Denisovan local ancestry in Oceanian (Australians, Papuans and Bougainville Islanders) populations. The method is a modification of the previously proposed CRF [S1] to improve the ability to deconvolve the contributions of Neanderthal and Denisovan ancestries (described in Section).

Denisovan date	Neanderthal date	Estimated Denisovan date	Estimated Neanderthal date	Neanderthal-Denisovan dates (Z-score)
1500	2000	1579.8±25.7	1924.1±40.5	7.2
2000	1500	2069.8±41.1	1555.9±30.8	-9.8
1800	2000	1881.0±33.0	1882.5±39.5	0
2000	1800	2106.1±43.0	1826.9±37.6	-4.8
1900	2000	1939.3±38.0	1924.4±45.9	-0.3
2000	1900	2018.5±39.2	1850.5±40.2	-3.1
2000	2200	1914.4±39.3	1943.1±34.6	0.5
2200	2000	2225.7±55.1	1773.9±30.37	-7.2

Table S1: Evaluation of Neanderthal and Denisovan admixture date estimates on simulated data (related to Figure 1). For every setting of the true Neanderthal and Denisovan dates, we show the Block Jackknife corrected point estimate and standard errors as well as the block Jackknife Z-score for the difference in the estimates. The top rows correspond to a simple demographic model while the bottom two rows correspond to data simulated under a demographic model based on the model used in [S2]

Populations	Neanderthal ancestry		Denisovan ancestry		Populations	Neanderthal ancestry		Denisovan ancestry	
	A (%)	X (%)	A (%)	X (%)		A (%)	X (%)	A (%)	X (%)
Abkhasian	0.976	0.100	0.011	0.000	Khonda Dora	1.207	0.157	0.086	0.000
Adygei	1.126	0.119	0.020	0.000	Kinh	1.448	0.433	0.052	0.000
Albanian	1.203	0.334	0.019	0.000	Korean	1.457	0.539	0.062	0.000
Aleut	1.357	0.368	0.044	0.000	Kurumba	1.313	0.751	0.081	0.000
Altaian	1.413	0.445	0.064	0.000	Kusunda	1.256	0.581	0.075	0.061
Ami	1.440	0.183	0.047	0.019	Kyrgyz	1.306	0.101	0.040	0.000
Armenian	1.077	0.121	0.013	0.000	Lahu	1.358	0.075	0.061	0.000
Atayal	1.531	0.785	0.062	0.000	Lezgin	1.125	0.338	0.014	0.019
Australian	1.559	0.300	0.895	0.105	Madiga	1.126	0.795	0.073	0.000
Balochi	1.070	1.046	0.026	0.000	Makrani	1.041	0.141	0.015	0.000
Basque	1.100	0.098	0.011	0.000	Mala	1.127	0.527	0.052	0.000
BedouinB	0.858	0.386	0.007	0.000	Mansi	1.311	0.091	0.040	0.000
Bengali	1.261	0.268	0.063	0.000	Maori	1.252	0.000	0.136	0.000
Bergamo	1.134	0.015	0.020	0.000	Mayan	1.386	0.183	0.069	0.000
Bougainville	1.622	1.375	0.861	0.032	Miao	1.341	0.151	0.073	0.000
Brahmin	1.101	0.635	0.064	0.000	Mixe	1.342	0.222	0.048	0.000
Brahui	1.099	0.261	0.018	0.000	Mixtec	1.252	0.414	0.044	0.000
Bulgarian	1.078	0.250	0.005	0.000	Mongola	1.389	0.346	0.068	0.000
Burmese	1.334	0.427	0.057	0.000	Nahua	1.332	0.263	0.046	0.000
Burusho	1.272	0.200	0.035	0.061	Naxi	1.371	0.106	0.070	0.000
Cambodian	1.419	0.538	0.075	0.000	North Ossetian	1.079	0.226	0.013	0.000
Chane	1.338	0.761	0.042	0.000	Norwegian	1.157	0.297	0.001	0.000
Chechen	1.019	0.000	0.025	0.000	Onge	1.325	0.533	0.057	0.000
Chipewyan	1.633	0.384	0.049	0.000	Orcadian	1.132	0.077	0.004	0.000
Chukchi	1.228	0.161	0.040	0.000	Oroqen	1.399	0.540	0.059	0.000
Cree	1.260	0.126	0.057	0.000	Palestinian	0.909	0.074	0.010	0.000
Crete	0.993	0.187	0.014	0.000	Papuan	1.596	0.366	1.123	0.269
Czech	1.067	0.000	0.028	0.000	Pathan	1.097	0.469	0.041	0.000
Dai	1.314	0.211	0.064	0.014	Piapoco	1.318	0.236	0.053	0.000
Daur	1.359	0.475	0.067	0.010	Pima	1.437	0.266	0.052	0.000
Druze	0.965	0.186	0.011	0.000	Polish	1.086	0.240	0.036	0.000
Dusun	1.438	0.312	0.086	0.000	Punjabi	1.156	0.156	0.061	0.000
English	1.085	0.210	0.015	0.000	Quechua	1.361	0.333	0.045	0.000
Eskimo Chaplin	1.500	0.000	0.053	0.000	Relli	1.190	0.572	0.064	0.019
Eskimo Naukan	1.401	0.408	0.060	0.000	Russian	1.148	0.243	0.018	0.000
Eskimo Sireniki	1.491	0.265	0.051	0.000	Saami	1.363	0.000	0.028	0.000
Estonian	1.076	0.167	0.021	0.000	Samaritan	0.888	0.000	0.002	0.000
Even	1.411	0.229	0.064	0.000	Sardinian	1.133	0.200	0.009	0.000
Finnish	1.165	0.302	0.013	0.000	She	1.468	0.224	0.077	0.000
French	1.023	0.188	0.012	0.000	Sherpa	1.395	0.250	0.106	0.000
Georgian	1.134	0.000	0.012	0.000	Sindhi	1.174	0.188	0.048	0.022
Greek	0.975	0.579	0.005	0.000	Spanish	1.031	0.130	0.018	0.000
Han	1.495	0.144	0.062	0.005	Surui	1.446	0.011	0.050	0.000
Hawaiian	1.342	0.184	0.117	0.000	Tajik	1.064	0.068	0.016	0.000
Hazara	1.225	0.324	0.034	0.000	Thai	1.458	0.584	0.048	0.000
Hezhen	1.399	0.277	0.053	0.000	Tibetan	1.389	0.169	0.082	0.010
Hungarian	1.122	0.057	0.019	0.000	Tlingit	1.261	0.211	0.042	0.000
Icelandic	1.237	0.147	0.015	0.000	Tu	1.466	0.232	0.045	0.000
Igorot	1.399	0.503	0.048	0.000	Tubalar	1.391	0.261	0.052	0.000
Iranian	0.968	0.351	0.022	0.000	Tujia	1.430	0.266	0.092	0.010
Iraqi Jew	0.926	0.231	0.020	0.000	Turkish	1.024	0.226	0.014	0.000
Irula	1.199	0.212	0.089	0.000	Tuscan	1.151	0.131	0.016	0.000
Itelman	1.428	0.042	0.045	0.000	Ulchi	1.508	0.177	0.064	0.000
Japanese	1.308	0.444	0.058	0.000	Uygur	1.170	0.398	0.057	0.019
Jordanian	0.810	0.282	0.005	0.000	Xibo	1.437	0.438	0.066	0.000
Kalash	1.113	0.409	0.025	0.000	Yadava	1.157	0.469	0.047	0.000
Kapu	1.069	0.705	0.055	0.000	Yakut	1.525	0.155	0.070	0.000
Karitiana	1.374	0.120	0.037	0.000	Yemenite Jew	0.947	0.277	0.012	0.000
Kashmiri Pandit	1.175	0.235	0.041	0.000	Yi	1.387	0.036	0.070	0.000
Kharia	1.133	0.380	0.085	0.000	Zapotec	1.360	0.329	0.051	0.000

Table S2: Summary of proportion of the genome confidently inferred to be archaic in ancestry (related to Table 1). Archaic ancestry estimates refer to the fraction of SNPs which have a marginal probability of either Neanderthal or Denisovan ancestry > 0.50 . The fraction of Neanderthal ancestry in individual i is estimated by the statistic $tia^{(n)}(i)$ while the fraction of Denisovan ancestry in individual i is estimated by $tia^{(d)}(i)$ (see Equation 1 in Section). We report the mean across individuals within each population and use a threshold of 0.50. A and X refer to estimates across the autosomes and X chromosome respectively.

Population	Region	<i>tia</i>	Z-score
Dai	East Asia	0.000642887	4.552016
Daur	East Asia	0.000665048	4.483456
Han	East Asia	0.000617295	4.39127
Japanese	East Asia	0.000580133	4.473346
Naxi	East Asia	0.000701322	4.644555
She	East Asia	0.000766465	4.230774
Xibo	East Asia	0.000660518	4.16324
Yi	East Asia	0.000701042	4.120488
Bengali	South Asia	0.000634354	4.110124
Sherpa	South Asia	0.00105782	4.737869
Tibetan	South Asia	0.000824393	4.136213
Eskimo_Naukan	Central Asia	0.000601988	4.080411
Even	Central Asia	0.000641474	4.61232
Australian	Oceania	0.00894954	9.019621
Bougainville	Oceania	0.0086141	8.616564
Hawaiian	Oceania	0.00117403	4.052288
Maori	Oceania	0.00136216	4.79091
Papuan	Oceania	0.0112295	10.79779

Table S3: Populations with a higher proportion of the genome confidently inferred to be Denisovan compared to French (related to Figure 2). We report populations where the difference in the confidently inferred proportion of Denisovan ancestry (*tia*) is statistically significant ($Z\text{-score} > 4$).

Table S4: Regions of elevated archaic ancestry proportion in American populations (related to Figure 3A). We report 100 kb non-overlapping windows with average marginal probability of archaic ancestry: $la \geq 0.30$). We report windows of elevated Neanderthal ancestry in Americans, Central Asians, East Asians, Oceanians, South Asians, and West Eurasians as well as windows of elevated Denisovan ancestry in Oceanians.

This table is provided as an Excel file.

GO term	America	Central Asia	East Asia	South Asia	West Eurasia	Oceania	Denisova
cellular response to cadmium ion		0.001	0.001	0.001			
cellular response to inorganic substance		0.001	0.001	0.012			
cellular response to metal ion		0.001	0.001	0.002			
cellular response to zinc ion		0.001	0.001	0.001			
chemokine-mediated signaling pathway				0.004			
cytokine production involved in inflammatory response					0.048		
glycosphingolipid metabolic process						0.002	
positive regulation of keratinocyte proliferation	0.012						
regulation of cytokine production involved in inflammatory response					0.023		
response to cadmium ion			0.017	0.001			
extracellular region					0.026		
intermediate filament	0.001	0.001					
intermediate filament cytoskeleton	0.001	0.012					
intracellular						0.005	
intracellular membrane-bounded organelle						0.015	
intracellular organelle						0.012	
intracellular part						0.008	
invadopodium						0.023	
keratin filament	0.001	0.001	0.001	0.001	0.036		
membrane-bounded organelle						0.023	
organelle						0.015	
cadmium ion binding			0.032	0.03			
C-C chemokine receptor activity				0.001			
chemokine receptor activity				0.001			
cytokine receptor activity				0.001			
G-protein coupled chemoattractant receptor activity				0.001			
phospholipid transporter activity							0.044
trace-amine receptor activity							0.001

Table S5: Gene Ontology categories with elevated archaic ancestry (related to Figure 3A). We list GO-categories that have significantly elevated archaic ancestry (FWER p-value < 0.05) grouped by biological process, cellular component and molecular function. We list categories that are significantly enriched for Neanderthal ancestry in each of six non-African groups as well as categories that are enriched for Denisovan ancestry in Oceanians (Papuan, Australians and Bougainville Islanders).

Population		ρ (se)	la $-\log_{10}(pval)$	ρ (se)	$ta_{0.25}$ $-\log_{10}(pval)$	ρ (se)	$ta_{0.9}$ $-\log_{10}(pval)$
Autosomes	East Asians	0.255 (0.0196)	38.063	0.0408 (0.0193)	1.461	-0.0294 (0.0181)	0.980
X	East Asians	0.379 (0.0688)	7.436	0.159 (0.0931)	1.061	0.146 (0.0933)	0.926
Autosomes	Oceanians	0.29 (0.0196)	48.752	0.0157 (0.0202)	0.361	-0.0234 (0.0192)	0.648
X	Oceanians	0.284 (0.0964)	2.499	-0.0193 (0.156)	0.045	-0.113 (0.143)	0.369
Autosomes	West Eurasians	0.252 (0.0169)	49.162	0.0448 (0.0162)	2.246	-0.0306 (0.0148)	1.419
X	West Eurasians	0.38 (0.079)	5.827	0.178 (0.0517)	3.239	0.138 (0.0509)	2.167
Autosomes	Oceanians	0.263 (0.018)	47.764	-0.029 (0.017)	1.053	-0.0647 (0.014)	5.405
X	Oceanians	0.333 (0.0906)	3.630	0.125 (0.193)	0.286	0.125 (0.173)	0.326

Table S6: Relationship between archaic ancestry and B-statistic (related to Figure 3C).

On top, relationship between Neanderthal ancestry and B-statistic for West Eurasians, East Asians and Oceanians (Australians, Papuans and Bougainville Islanders). On bottom, relationship between Denisovan ancestry and B-statistic in Oceanians (Australians, Papuans and Bougainville Islanders) on the autosomes and the X chromosome. ρ refers to Spearman's correlation coefficient, la , $ta_{0.9}$ and $ta_{0.25}$ refer to different summaries of archaic ancestry. We show results on autosomes and X chromosome.

Tissue	Uncorrected			B-statistic						Heterozygosity					
	A+X	A	X	A+X		A		X		A+X		A		X	
				Mean $\times 10^{-4}$	<i>p</i>	Mean $\times 10^{-4}$	<i>p</i>	Mean $\times 10^{-4}$	<i>p</i>	Mean $\times 10^{-4}$	<i>p</i>	Mean $\times 10^{-4}$	<i>p</i>	Mean $\times 10^{-4}$	<i>p</i>
Adipose	0.8	0.75	0.98	724	0.67	728	0.61	738	0.92	11	0.73	11	0.69	10	0.89
Adrenal	0.74	0.69	1	736	0.56	732	0.53	NA	NA	12	0.66	11	0.61	NA	NA
Blood	0.93	0.92	0.34	722	0.77	722	0.75	679	0.5	9.7	0.92	9.6	0.91	10	0.5
Brain	1	1	0.2	685	1	692	1	685	0.22	9.1	1	9.1	1	10	0.14
Breast	0.53	0.47	0.96	728	0.35	733	0.32	644	0.78	12	0.43	12	0.38	9.3	0.86
Colon	0.28	0.28	0.8	695	0.23	702	0.22	718	0.5	9.9	0.24	9.9	0.23	10	0.5
Heart	0.95	0.94	0.76	668	0.96	668	0.95	725	0.5	9.6	0.95	9.5	0.94	9.6	0.49
Kidney	0.71	0.7	0.64	677	0.7	677	0.67	667	0.5	10	0.67	10	0.66	9.4	0.5
Liver	0.39	0.24	0.98	662	0.51	660	0.36	673	0.96	9.9	0.36	9.9	0.22	9.6	0.96
Lung	0.82	0.77	0.91	723	0.65	715	0.6	659	0.8	12	0.74	12	0.69	9.6	0.75
Lymph	0.91	0.91	0.9	675	0.9	665	0.88	753	0.5	9.9	0.89	9.6	0.88	11	0.5
Ovary	0.13	0.12	0.9	755	0.05	736	0.049	642	0.5	10	0.1	9.8	0.095	8.4	0.5
Prostate	0.64	0.59	0.95	754	0.41	756	0.38	778	0.5	10	0.58	11	0.53	9.4	0.5
Skeletal muscle	0.56	0.44	0.95	600	0.91	600	0.84	672	0.94	9	0.56	8.9	0.44	9.7	0.89
Testes	1.2e-07	6e-06	0.46	673	4.4e-07	672	1.7e-05	682	0.046	9.2	3.2e-07	9.4	9.6e-06	9.6	0.3
Thyroid	0.73	0.7	0.9	724	0.59	718	0.56	657	0.5	10	0.68	10	0.65	11	0.5
Adipose	0.26	0.17	0.93	724	0.18	728	0.11	738	0.84	11	0.19	11	0.12	10	0.79
Adrenal	0.85	0.86	1	736	0.77	732	0.78	NA	NA	12	0.78	11	0.8	NA	NA
Blood	0.058	0.037	0.91	722	0.029	722	0.015	679	0.88	9.7	0.056	9.6	0.037	10	0.87
Brain	0.97	0.94	0.98	685	0.97	692	0.92	685	0.98	9.1	0.98	9.1	0.95	10	0.98
Breast	0.65	0.68	0.62	728	0.54	733	0.56	644	0.37	12	0.52	12	0.56	9.3	0.34
Colon	0.91	0.87	0.97	695	0.89	702	0.83	718	0.91	9.9	0.89	9.9	0.84	10	0.89
Heart	0.83	0.88	0.3	668	0.82	668	0.88	725	0.49	9.6	0.81	9.5	0.87	9.6	0.49
Kidney	0.79	0.83	0.46	677	0.77	677	0.81	667	0.29	10	0.75	10	0.8	9.4	0.29
Liver	0.72	0.7	0.83	662	0.76	660	0.76	673	0.76	9.9	0.7	9.9	0.68	9.6	0.75
Lung	0.89	0.87	0.85	723	0.82	715	0.79	659	0.75	12	0.81	12	0.79	9.6	0.76
Lymph	0.96	0.97	0.62	675	0.95	665	0.97	753	0.49	9.9	0.95	9.6	0.97	11	0.49
Ovary	0.15	0.18	0.62	755	0.089	736	0.11	642	0.49	10	0.12	9.8	0.14	8.4	0.49
Prostate	0.24	0.26	0.78	754	0.15	756	0.17	778	0.49	10	0.19	11	0.22	9.4	0.49
Skeletal muscle	0.68	0.68	0.71	600	0.83	600	0.86	672	0.6	9	0.69	8.9	0.69	9.7	0.59
Testes	2.2e-03	6.8e-03	0.015	673	2.8e-03	672	8.8e-03	682	4e-03	9.2	2.9e-03	9.4	7.8e-03	9.6	6.7e-03
Thyroid	0.37	0.42	0.62	724	0.27	718	0.31	657	0.49	10	0.3	10	0.35	11	0.49
Adipose	0.088	0.053	0.93	724	0.025	728	0.011	738	0.84	11	0.039	11	0.024	10	0.8
Adrenal	0.6	0.51	1	736	0.38	732	0.32	0	0	12	0.4	11	0.34	0	0
Blood	0.93	0.84	0.87	722	0.63	722	0.43	679	0.86	9.7	0.92	9.6	0.83	10	0.82
Brain	1	1	0.98	685	1	692	0.99	685	0.98	9.1	1	9.1	1	10	0.98
Breast	0.85	0.82	0.85	728	0.66	733	0.64	644	0.71	12	0.67	12	0.67	9.3	0.68
Colon	0.27	0.15	0.98	695	0.18	702	0.082	718	0.93	9.9	0.22	9.9	0.12	10	0.91
Heart	0.6	0.55	0.38	668	0.66	668	0.61	725	0.24	9.6	0.57	9.5	0.53	9.6	0.24
Kidney	0.93	0.97	0.022	677	0.93	677	0.96	667	0.49	10	0.89	10	0.94	9.4	0.49
Liver	0.83	0.71	0.55	662	0.94	660	0.9	673	0.46	9.9	0.74	9.9	0.64	9.6	0.44
Lung	0.88	0.8	0.87	723	0.64	715	0.53	659	0.79	12	0.84	12	0.76	9.6	0.8
Lymph	0.63	0.67	0.39	675	0.62	665	0.63	753	0.49	9.9	0.57	9.6	0.62	11	0.49
Ovary	0.37	0.3	0.86	755	0.13	736	0.092	642	0.65	10	0.3	9.8	0.24	8.4	0.64
Prostate	0.83	0.79	0.62	754	0.55	756	0.52	778	0.49	10	0.76	11	0.73	9.4	0.49
Skeletal muscle	0.58	0.38	0.94	600	0.99	600	0.96	672	0.92	9	0.68	8.9	0.47	9.7	0.91
Testes	3.6e-09	3.1e-05	0.0086	673	6.7e-09	672	7.7e-05	682	0.0011	9.2	1.9e-08	9.4	5e-05	9.6	0.004
Thyroid	0.54	0.43	0.86	724	0.32	718	0.24	657	0.66	10	0.42	10	0.35	11	0.63

Table S7: Enrichment of tissue-expressed genes in regions of the genome depleted in Denisovan ancestry (top), Neanderthal ancestry (middle) in Oceanians populations and Neanderthal ancestry in mainland Eurasians (bottom) (related to Figure 3C). We compare tissue-expressed genes (defined as genes that are more significantly expressed in a given tissue compared to all other tissues) to all genes that are specific to at least one tissue. We report the one-sided *P*-value for Fisher’s exact test for the genes on the autosomes, X chromosomes and for the combined set across autosomes and X chromosomes. Only testes-expressed genes remain statistically significantly enriched in regions with low Denisovan ancestry after correcting for 16 tests in each case (highlighted). We also repeated this analysis correcting for the B-statistic and for the local heterozygosity from a panel of Africans. We report the one-sided value of a test of the coefficient associated with a gene being present in a given tissue in a logistic regression of the depletion status of a genes that also included as a covariate the B-statistic or the local heterozygosity. Local heterozygosity for each gene is calculated across 76 African chromosomes, restricting to sites which pass filter level ≥ 1 , and to sites where at least half the samples have a valid genotyping call. Samples from panel A were excluded as the error rate is known to be higher. Only testes-expressed genes show a statistically significant enrichment in regions with low archaic ancestry. Oceanian populations refer to Papuans, Australians and Bougainville Islanders. A - autosomes, X - X chromosomes, A+X - combined autosomes and X chromosome, Mean - mean of the B-statistic or the heterozygosity across the class of genes examined, *p* - *P*-value for Fisher’s exact test. We note that adipose-expressed and blood-expressed genes appear to be nominally depleted for Neanderthal ancestry in mainland Eurasians and Oceanians respectively though the corresponding *P*-values are not significant after multiple testing correction.

Supplemental Experimental Procedures

Estimating the date of archaic gene flow into Oceanian populations

As a first step towards understanding the history of Denisovan gene flow into the Oceanian populations, we need to infer the date of this gene flow event (or more precisely, the date of last exchange of genes between the ancestral populations). To do this, we will measure the extent of admixture linkage disequilibrium (LD) (such a statistic was used to estimate Neanderthal gene flow in Europeans [S3]). A limiting factor in estimating accurate dates of admixture events that are more than thousands of years old is the accuracy of the genetic maps used. To estimate dates accurately, [S3] developed a procedure to correct the nominal LD-based dates using estimates of the error of genetic maps. In turn, the errors in a given genetic map were estimated by comparing the map to crossovers observed in a European pedigree [S4]. Alternately, the error in the map could be assessed within the statistical framework used to estimate map. However, this procedure limits the applicability of LD-based admixture date estimation as it requires access to both a population-specific map as well as an estimate of the error associated with the map.

Rather than attempt to estimate absolute dates (which requires us to characterize the errors in the genetic maps), we attempt to obtain a relative ordering of Neanderthal and Denisovan admixture events. Given that Oceanian populations have a history of gene flow from populations related to Neanderthals as well as Denisovans, we can ask if Denisovan gene flow event pre or post-dated the Neanderthal gene flow event (we use the term gene flow to refer to the date of last exchange of genes – it is possible and quite likely that there were multiple episodes of gene flow or a period of continuous gene flow between two populations). Since we are estimating the date of gene flow in the same population, it is meaningful to compare these dates.

Our procedure for dating gene flow in a target population begins by ascertaining a set of SNPs. For all pairs of ascertained SNPs at a given genetic distance x , we compute $C(x)$ defined to be the average of Lewontin’s D in the target population. We then fit an exponential function to $C(x)$ as a function of x using ordinary least squares for x in the range of 0.02 cM to 1 cM and use the rate of decay as an estimate of the time of gene flow. To estimate standard errors of this estimate, we use a weighted Block Jackknife [S5] with 10 Mb blocks having a minimum of 100 SNPs.

To estimate the date of Neanderthal gene flow in a test population, we ascertain SNPs at which a single randomly chosen Neanderthal allele (from a diploid Neanderthal genome) is derived relative to the human-chimp ancestor, a single randomly chosen Denisovan allele is ancestral, all alleles in a panel of sub-Saharan Africans are ancestral and that are polymorphic in the test population. We term this ascertainment $nd10$. For the Neanderthal and Denisovan alleles, we use the diploid genotypes from the high-coverage Altai Neanderthal genome [S6] and Denisovan genome [S7] respectively. For the sub-Saharan Africans, we use a panel of 44 high-coverage genomes sequenced as part of the Simons Genome Diversity Project (SGDP) [S8] that we determined are closely related to the Yoruba relative to Altai Neanderthal (see for details on processing of SGDP data). More precisely, we included all populations such that the Z-score of the D-statistic $D(X, Yoruba; Neanderthal, Chimp)$ is less than 2, where X is one of n African populations sequenced in the SGDP. We computed this D-statistic restricting to transversions.

To estimate the date of Denisovan gene flow, we ascertain SNPs at which Denisova is derived and Neanderthal is ancestral and all sub-Saharan Africans are ancestral ($nd01$). For the genetic map, we used the combined Oxford LD-based map [S9].

Our test panel consists of individuals from Papua New Guinea, Aboriginal Australians and Bougainville islanders (16 Papuans, 2 Australian Aborigines and 2 Bougainville islanders).

We estimate the nominal time of gene flow λ in Oceanians as $\lambda = 1121 \pm 16$ for Neanderthal gene flow and $\lambda = 1000 \pm 8$ for Denisovan gene flow. Thus, the nominal date of last exchange of genes

between Denisovans and Oceanians postdates the corresponding date for Neanderthals and Oceanians (Block Jackknife two-sided P-value 4.3×10^{-5}). This date is consistent with a model in which Denisovan gene flow occurred after the divergence of these populations from other Eurasian populations.

It is plausible that there were multiple introgression events associated with either archaic so that a single pulse of admixture is not a good model. To test this, we fit a model that is a mixture of two exponentials. For Neanderthal gene flow, we estimate nominal admixture dates of $\lambda_1 = 1197$, $\lambda_2 = 90262$. For Denisovan gene flow, we estimate $\lambda_1 = 986$, $\lambda_2 = 21808$. Thus, our estimates are relatively insensitive to the assumption of one vs two pulses of admixture. Further, in both the Neanderthal and Denisovan gene flow events, the older date is substantially older (at least 20 times) and at least as old as the split times of the archaics from modern humans suggesting little evidence for additional older admixture events since the split of archaic and modern human populations.

Simulations

To test the robustness of our results, we performed coalescent-based simulations under a demographic model in which a present-day non-African population had gene flow from both Neanderthals and Denisovans.

We generated 3000 independent 1 Mb regions. We set the mutation rate to $1.2e - 8$ and the recombination rate to $1.3e - 8$. We simulated 100 Oceanian and African chromosomes and 1 Neanderthal and Denisovan chromosome. All effective population sizes were fixed at 10000. We set the Archaic-modern human split, Neanderthal-Denisovan split, and African-non-African split to 12000, 8000 and 2500 generations respectively. The Neanderthal and Denisovan mixture proportions were set to 2% and 4.5% respectively. We fixed the time of the older admixture event to 2000 generations and varied that of the more recent admixture event across 1500, 1800 and 1900 generations. For each parameter instantiation, we considered a setting where the Neanderthal admixture pre-dated the Denisovan admixture and vice-versa. Table S1 shows the estimated dates. We see that the estimates are unbiased when the difference between the admixture dates is at least 500 generations. As the difference decreases, estimates of the older dates in particular tend to be biased. This bias tends to affect the Neanderthal estimate more than the Denisovan estimate. This is likely an effect of the smaller Neanderthal admixture proportion that leads to a noisier LD decay signal. However, the relative order of dates is always consistent. We computed a block Jackknife difference for a difference in the two estimates. In the cases where the null of no difference was rejected, the direction of the difference is consistent with the direction of the difference of the two parameters. There appears to be less power to reject the null in the cases where the Neanderthal admixture is older than the Denisovan admixture. We note that the power of this test is expected to be higher in simulations than in real data due to the fact that we simulate independent 1 Mb long regions so that the simulations carry more independent loci than real data.

We performed an additional set of simulations using a more realistic demographic model. We do not have a detailed joint demographic model relating Oceanians, Neanderthals and Denisovans. Instead, we modified the demographic model of non-Africans and Neanderthals used in [S2] that is, in turn, based on a demographic model fit by [S10]. We used the East Asian demographic parameters as a proxy for the Oceanian populations. We added both Neanderthal and Denisovan populations to this model. Neanderthal and Denisovan admixture proportions were set to 2% and 4.5% respectively. The split time of the two archaics was set to 8000 generations with their effective population sizes set to 2500 as was done in [S2]. We also modeled the observation [S6] that the divergence of the introgressing and sequenced Denisovans is larger than that of Neanderthals by setting these split times to 5600 and 2800 generations for Denisovans and Neanderthals respectively. We considered a model where the Neanderthal and Denisovan admixture dates are 2000 and 2200 generations respectively as well as one where the Denisovan admixture occurred earlier. Table S1 again shows that our estimates detect a statistically significant difference in the correct direction when the Denisovan admixture pre-dates Neanderthal admixture. However, in the opposite setting, the difference is no longer significant though the difference of the point estimates has

the same sign as that of the true parameter values.

These simulations indicate that our estimate of the relative dates of archaic admixture is robust although the absolute estimates themselves are quite sensitive (both to demographic parameters as well as to errors in the genetic map that we have not considered here but have been shown to affect these statistics previously [S3]).

Maps of archaic ancestry in diverse present-day humans

To infer maps of Neanderthal and Denisovan ancestry, we first applied a Conditional Random Field that had previously been developed to infer Neanderthal ancestry in Eurasian populations [S1]. The CRF used in [S1] was designed to infer archaic ancestry in populations that have a single dominant archaic ancestry component. While the inference from this application are reasonable for populations with a single dominant archaic component, we propose a modified method in Section that we show has improved accuracies for populations that have both Neanderthal and Denisovan ancestries.

To infer Neanderthal (Denisovan) ancestry, we applied the CRF using the high-coverage Altai Neanderthal [S6] (the high-coverage Denisovan genome [S7]) as an archaic reference (essentially, performing two two-way classifications). Inferences in the CRF require us to estimate model parameters. We fixed the model parameters to the values estimated in [S1].

We applied the CRF to present-day human genomes from diverse populations that were sequenced as part of the Simons Genome Diversity Project (SGDP) combined with genomes from the panel A individuals sequenced in an earlier study [S6]. The sequencing reads for the panel A individuals were processed using the same pipeline as the SGDP. We grouped the individuals according to five continental populations: West Eurasians, East Asians, Oceanians, South Asians, Americans and Central Asians. Of particular interest in this dataset are the populations that harbor a substantial fraction of Denisovan ancestry. To study these populations, we considered a subset of the Oceanian populations – Australians, Papuans and Bougainville Islanders, that consists of 16 individuals from Papua New Guinea, 2 from Bougainville Islands and 2 Australian Aborigines.

We used 43 African genomes from 17 populations as a reference panel of modern humans assumed to carry no archaic ancestry. These genomes were chosen from populations that are similar to the west African Yoruba (YRI) in their relationship to the Altai Neanderthal, *i.e.*, we chose populations X for which the Z-score associated with the D-statistic, $D(X, YRI; Altai\ Neanderthal, Chimpanzee)$ is less than two (where the standard error of the D-statistic is estimated using a weighted block jackknife with 5 cM blocks [S11]).

To infer Denisovan ancestry, we constructed two reference panels: one panel consists of the Denisovan genome [S7] sequenced to 31-fold coverage while the other consists of the 43 African genomes [S6]. To infer Neanderthal ancestry, one of the reference panels consists of the Altai Neanderthal genome [S6] sequenced to 52-fold coverage while the other consists of the 43 African genomes. For each haplotype $i \in \{1, \dots, I\}$ in the target population and SNP $s \in \{1, \dots, S\}$, we apply the CRF to estimate $\gamma_{i,s}^{(n)}$ and $\gamma_{i,s}^{(d)}$ – the marginal probabilities of Neanderthal and Denisovan ancestry at SNP s of haplotype i .

Data Processing

Genotypes were called using the procedure described in [S8]. Briefly, BWA-MEM [S12] alignments were used as input for single-sample genotype calls using a reference-bias-free modification of the Unified Genotyper from the Genome Analysis Toolkit (GATK) [S13]. Sites which were found to be both polymorphic in at least one sample compared with chimpanzee and which pass filters (at filter level 1) were compiled (62.6M sites). At these discovered positions, genotype calls for samples were compiled at filter level 0 (the lower filter level is justified as the sites are known to be polymorphic in at least one sample).

We applied previously described filters to the Altai Neanderthal genome [S6] and the Denisovan genome [S7]. These filters restrict to sites that are non-repetitive, uniquely mappable and are not outliers with respect to coverage. Due to the high-coverage of these genomes, we work directly with the genotypes called from the ancient DNA reads (using GATK [S13]). This reduces the effects of genotyping errors as well as contamination (which is estimated to be at 1% at the read-level and hence substantially smaller at the genotype level for either of the genomes).

We restricted to SNPs that are biallelic across chimpanzee, ancient and modern genome sequences. We also filtered sites at which more than half the African reference genotypes are missing as well as sites where the Neanderthal or Denisovan genotype is missing.

The CRF requires phased genomes as input. We simultaneously phased all the genotypes in SGDP and panel A using SHAPEIT with default parameters [S14]. The ancestral allele at each site was determined from the 1000 Genomes ancestral sequence. Genetic distances were obtained from the combined LD map [S9] lifted over to hg19 coordinates. For the X chromosome, we obtained a sex-averaged map by scaling the X chromosome LD-based map by $\frac{2}{3}$.

Genome-wide analysis of archaic ancestry

For each individual i and archaic ancestry $a \in \{n, d\}$, we estimated the proportion of the genome that is confidently inferred to harbor archaic ancestry, $tia^{(a)}(i)$, to be the fraction of SNPs for which the marginal probability $\gamma_{i,s}^{(a)} > 0.90$.

$$tia^{(a)}(i) = \frac{1}{|H(i)|} \sum_{h \in H(i)} \frac{\sum_{s=1}^S \mathbf{1}\{\gamma_{i,s}^{(a)} > 0.90\}}{S} \quad (1)$$

We will drop the superscript when the archaic ancestry being referred to is clear from context. Here $H(i)$ indexes the haplotypes that belong to individual i . The above equation also holds for estimating Neanderthal ancestry on the X chromosome. In the case of the X chromosome, we average over both chromosomes for females only.

Empirical estimate of the accuracy of archaic ancestry estimates

We can estimate the accuracy of the archaic ancestry estimates on the SGDP data under several assumptions. The basic idea is as follows: the inferred Neanderthal ancestry in a target population can be modeled as arising from a process that classifies true Neanderthal, Denisovan or modern human alleles as Neanderthal. Given previous estimates of the Neanderthal and Denisovan ancestry in the target population, we can estimate these classification probabilities. These classification probabilities, in turn, provide information on the accuracy of the inference. For example, the proportion of Neanderthal ancestry inferred in a population like the African hunter-gatherers gives us the probability that a modern human allele is classified as Neanderthal assuming that the African hunter-gatherers have neither Neanderthal nor Denisovan ancestries. The procedure that we describe integrates out the uncertainty in the true Neanderthal and Denisovan ancestries across populations to estimate classification probabilities which in turn can be converted into estimates of precision and recall.

In these analyses, we will consider African hunter-gatherers (Khomani San), West Eurasians, East Asians and Oceanians. For SNPs that are assigned a marginal probability $\geq t$, let $p_{i,j}(t)$, $i, j \in \{n, d, m\}$ denote the probability of that an allele of ancestry i was assigned ancestry j , where the ancestries $\{n, d, m\}$ refer to Neanderthal, Denisovan and modern human ancestries respectively. We assume that these probabilities are constant across the populations analyzed. This assumption holds if the Neanderthal and Denisovan ancestries in these populations are derived from similar ancestral populations and if the demographic histories of these populations do not affect the accuracy of the CRF. The first assumption is reasonable given the close relatedness of existing Neanderthal genomes obtained from a

wide range of spatial and temporal separation [S6]. This assumption might also be violated if the archaic admixtures occurred at different times across populations. For Neanderthal ancestry, current estimates strongly suggest that most of the Neanderthal ancestry in non-African populations traces its origin to a shared admixture event (eastern non-Africans have about 25% more Neanderthal ancestry than west Eurasians [S6; 15]). Further, we have shown previously that the precision of our method changes by about 1% when the time of Neanderthal admixture varies across more than 1000 generations [S1] so that we expect these probabilities to be relatively robust to variation in the time of admixture. Another reason to expect that the assumption of constant probabilities might not hold is that the target populations differ in their recent demographic histories. Nevertheless, our method analyzes single haploid genomes in each of these populations and hence, should be robust to these differences. Further, since we are analyzing non-African genomes relative to archaic and African genomes, genomes from distinct non-African populations should show similar relationships to the African and archaic genomes. Non-African populations that have substantial African-related gene flow might violate this assumption. The African hunter-gatherer might appear to also violate these assumptions given that they might share recent ancestry with the African reference genomes.

Let $f_{i,k}$, $i \in \{n, m, d\}$, $k \in \{san, we, ea, me\}$ denote the true proportions of ancestry i in population k . For a given threshold t , we observe $\tilde{f}_{n,k}(t)$, $\tilde{f}_{d,k}(t)$, the fraction of sites with marginal probability of Neanderthal and Denisovan ancestry of at least t in population k . We can then find $p_{i,j}(t)$ by solving the following optimization problem.

$$\{p_{i,a}^*(t)\} = \underset{0 \leq p_{i,a}(t) \leq 1}{\operatorname{argmin}} \sum_{a \in \{n,d\}, k \in \{san, we, me, ea\}} \left(\tilde{f}_{a,k}(t) - \sum_{i \in \{d,m,n\}} f_{i,k} p_{i,a}(t) \right)^2$$

The precision (proportion of archaic ancestry called at threshold t that is true) for the estimates of archaic ancestry a in target population k is given by $p_{a,a}^*(t)$ while the recall (proportion of true archaic ancestry that is called at threshold t) is given by $\frac{f_{a,a} p_{a,a}^*(t)}{\sum_{i \in \{d,m,n\}} f_{i,k} p_{i,a}^*(t)}$. By computing these estimates for all values of $t \in [0, 1]$, we can estimate a precision-recall curve for each archaic ancestry estimate in a given population.

Since the true values of mixture proportions $f_{i,k}$ are not known, we sampled 100 times from the range of plausible values estimated for these quantities and averaged our precision and recall estimates over these samples. Specifically, we assumed $f_{n,san} = f_{d,san} = 0$, $f_{n,ea} = f_{n,me} \sim \mathcal{N}(0.0189, (0.0013)^2)$, $f_{n,we} = r f_{n,ea}$, $r \sim \mathcal{N}(0.76, (0.06)^2)$, $f_{d,we} = 0$, $f_{d,ea} \sim \operatorname{Unif}(0, 0.002)$ and $f_{d,me} \sim \operatorname{Unif}(0.03, 0.06)$. In words, we assume that the African hunter-gatherers have no archaic ancestry, West Eurasians have no Denisovan ancestry, East Asians and Oceanians have the same proportion of Neanderthal ancestry, Oceanians have substantial Denisovan ancestry while East Asians have a small fraction and that West Eurasians have slightly less Neanderthal ancestry than East Asians (consistent with previous studies). The use of the normal distribution for Neanderthal ancestry in West Eurasians and East Asians is motivated by the fact that these estimates are endowed with formal standard errors. We use a uniform distribution for the other estimates.

This procedure reveals that in populations such as West Eurasians and East Asians, which are well-modeled as a two-way admixture between modern and archaic humans, the CRF attains reasonable recall at high precision (attaining recalls $> 50\%$ at precisions $> 95\%$). However, as the Oceanians have substantial Neanderthal and Denisovan ancestries, the precision tends to be substantially lower (less than 80% for any recall). Further insight into the error processes can be obtained by inspecting the classification probabilities $p_{i,j}^*(t)$. For example, at a probability threshold $t = 0.90$, the probability of classifying an allele of modern human ancestry as either Neanderthal or Denisovan ($p_{m,n}^*(0.90)$ and $p_{m,d}^*(0.90)$) is of the order of 10^{-4} while the probability of classifying a Neanderthal allele as Denisovan

or vice-versa ($p_{n,d}^*(0.90)$ or $p_{d,n}^*(0.90)$) is of the order of 0.10 which is of the same order of magnitude as the probability that a Neanderthal (or Denisovan) allele is classified correctly ($p_{n,n}^*(0.90)$ or $p_{d,d}^*(0.90)$).

An improved procedure for deconvolving Neanderthal and Denisovan ancestries

We considered a modified procedure to improve the accuracy of archaic ancestry inference.

Firstly, we modified the reference panels. To infer Denisovan ancestry, we constructed two reference panels: one panel consists of the Denisovan genome while the other consists of 43 African genomes pooled with the Neanderthal genome. Analogously, to infer Neanderthal ancestry, one of the reference panels consists of the Neanderthal genome while the other consists of African and Denisovan genomes. A second modification we made is to set the model parameter associated with haplotypic feature to zero because we discovered a small bias induced by this parameter for populations with proportions of archaic ancestry that are of the order of $\frac{1}{1000}$. The bias arises because the CRF was trained to estimate ancestries of the order of 1/100 leading to a specific weighting of the haplotype parameter relative to the SNP parameters. This weighting is not appropriate when the true admixture fraction is substantially different. As a result, the method infers similar proportion of Denisovan ancestry in French and Han Chinese ($\approx 0.6\%$) in contradiction to [S1]. This modification allows the CRF to be applied to study Denisovan ancestries in mainland Eurasia.

We estimated the empirical accuracy of this modified procedure as described in Section . At a nominal probability threshold of 0.90, the CRF now attains a recall of around 47% at a precision of 97% for Neanderthal ancestry inference in West Eurasians and East Asians (Figure S1a). In Oceanians, it attains a recall of around 43% at a precision of 83% for Neanderthal ancestry and a recall of 14% at a precision of 97% for Denisovan ancestry (Figure S1b).

Given the relatively high precision of these estimates as well as the profile of the precision-recall curves that suggest that the precision remains high for lower probability thresholds, we chose a marginal probability threshold of 0.50 to call a SNP as archaic. At this threshold, the CRF has a recall of around 72% at precisions of around 97%, 97% and 85% respectively for Neanderthal ancestry in West Eurasians, East Asians and Oceanians whereas for Denisovan ancestry in Oceanians, the recall is around 24% at a precision of 97%. Our power to detect Denisovan ancestry in Oceanian populations is still lower than the power to detect Neanderthal ancestry. A likely explanation for this reduced power is the substantially larger divergence of the sequenced and introgressing genomes for the Denisovans compared to the Neanderthals [S6]. While the quantitative estimates of accuracy obtained in this framework depend on several assumptions about the distributions of archaic ancestries, the qualitative conclusion is that discriminating between distinct archaic ancestral components in a population such as Oceanians is challenging.

We can again obtain additional insights into the accuracy of our estimates by inspecting the classification probabilities $p_{,,}^*$. The probability of classifying a modern human allele as archaic is of the order of 10^{-4} or smaller, in the modified procedure (specifically, we estimate $p_{m,n}^*(0.50) = 2 \times 10^{-4}$, $p_{m,d}^*(0.50) = 4 \times 10^{-5}$). On the other hand, the probability of classifying one archaic allele as another is of the order of 0.01 (specifically, $p_{d,n}^*(0.50) = 0.05$, $p_{n,d}^*(0.50) = 0.01$), reduced relative to the method analyzed in Section . As a result, there is an increased probability that an allele classified as Denisovan is truly Denisovan, particularly in populations that have substantial Neanderthal ancestry. These observations hold across a wide range of thresholds on probability t (including at $t = 0.25$, $t = 0.50$ and $t = 0.90$). Further, $p_{d,n}^* > p_{n,d}^*$ at these values of t , *i.e.*, our procedure is more likely to misclassify a Denisovan allele as Neanderthal than vice-versa. Thus, these classification probabilities tell us why the power or recall for Denisovan ancestry inference is lower than that for Neanderthal ancestry inference for the same probability threshold. This result is consistent with the larger divergence of sequenced and introgressing genomes for Denisovans relative to Neanderthals. Further, these probabilities also provide insight into why the

precision for Neanderthal ancestry inference in Oceanians is lower than that for Neanderthal ancestry inference in other non-Africans as well as for Denisovan ancestry inference in Oceanians. This observation is likely due to the higher rate of misclassification of Denisovan alleles as Neanderthal compared to the reverse process in combination with the higher proportion of Denisovan ancestry in Oceanians.

Variation in the genome-wide proportions of archaic ancestry

To formally test for differences in archaic ancestry, we tested for a difference in the *tia* statistic (Equation 1) across pairs of populations. Specifically, for a reference population r and a target population t , we computed $\delta(r, t) = tia(t) - tia(r)$. We assessed statistical significance using a block jackknife with 10 Mb blocks [S11].

Apart from Oceania, several populations in East, South, and Central Asia have higher values of *tia* for Denisovan ancestry (Table S3). For example, while the French have a mean *tia* of 0.01%, the Han have a mean *tia* of 0.06% (Z-score of 4.35). These proportions are rather small: the East Asian proportion of the genome called as Denisovan is about 5.8% of the corresponding proportion for Oceanians. Among the populations with elevated *tia* compared to French are the Tibetans and the Sherpa. The increased ancestry in the Sherpa and Tibetan populations is interesting in light of the evidence for Denisovan introgression at the EPAS1 locus that contributed to high-altitude adaptation in these populations [S16]. One possible explanation is that the increased ancestry is caused by Denisovan introgression at the EPAS1 locus. To test this explanation, we computed the *tia* statistic after removing chromosome 2 that contains the EPAS1 locus. We find that the *tia* statistic is highly concordant whether or not we include chromosome 2 ($\rho = 0.968$). Sherpa remains the population with the highest *tia* in both analyses while the ranks of the Tibetans are 7 and 5 depending on whether we include or exclude chromosome 2. Finally, we do not detect statistically significant increases (Z-score > 4 correcting for the multiple hypotheses tested) in Denisovan ancestry relative to Han Chinese within mainland Eurasians. We study this variation in more detail in Section .

Modeling the variation in Denisovan ancestry across populations

To understand how variation in Denisovan ancestry might be related to known population relationships, we tried to model the proportion of the genome inferred to be Denisovan in a given mainland Eurasian population as a linear function of its proximity to non-West Eurasians. Specifically, given that East Asians have higher Denisovan ancestry relative to West Eurasians, we asked if the Denisovan ancestry proportion in other mainland Eurasians can be explained by differential proportions of non-West Eurasian ancestries in these populations. For each mainland Eurasian population X , we computed the f_4 -statistic $f_4(X, Yoruba; Australian, Ust' - Ishim)$ which measures the drift shared by population X with East Eurasians since their split from the ancestors of West Eurasians. We then regressed an estimate of Denisovan ancestry against this f_4 statistic measured on West Eurasian and East Asian populations, *i.e.*, we learned the parameters of the regression on West Eurasians and East Asians. We then used this regression to predict the mean Denisovan ancestry in the other Eurasian populations. Figure 2(B) shows the Denisovan ancestry inferred by the CRF versus the Denisovan ancestry expected under the model. In American, central and south Asian (that includes populations such as the Sherpa) populations, the proportion of Denisovan ancestry is positively correlated with the f_4 statistic (Pearson’s correlation $\rho_{Pearson} = 0.832$, $Z = 6.27$).

We also observe that American, central and South Asian populations have systematically higher proportions of Denisovan ancestry than predicted by the linear model – the mean of the residuals is 1.36. Testing this model which involves a test of the residuals having mean zero presents two challenges: i) the analyzed populations are not independent observations as they share drift to various degrees, and ii) the estimates of both ancestries and the f_4 statistics are noisy. To test the model, we computed block jackknife standard errors for the mean of the residuals as well as the f_4 statistics. We deleted a

10 Mb block of the genome, in turn, and then computed Jackknife estimates of the Denisovan ancestry proportion and the f_4 statistics. We then ran the estimation procedure on the Jackknife estimates and computed the mean of the residuals on the American, central and South Asian populations. The Z-score for the mean of the residuals is 2.84 using the ancestry estimates from the CRF. An additional concern is that a handful (four) of the West Eurasian and East Asian populations used for parameter estimation appear to be outliers to the linear model (absolute value of standardized residuals > 2). We reran the inference after excluding these outliers and found that the results became more significant. We estimated Z-scores of 3.74 for the CRF.

To further narrow down this signal of increased Denisovan ancestry, we inspected the residuals for each population. For the ancestries estimated by the CRF, none of the residuals is individually significant. However, when we ranked the populations according to their residuals, we find that the south Asian populations are ranked highest. We reran the block jackknife testing the mean of the residuals in south Asians, central Asians and Americans. The Z-scores are 3.20, 1.21 and 0.13 for south Asians, central Asians and Americans respectively with the CRF estimates.

Coverage of archaic haplotypes

We defined archaic haplotypes as runs of consecutive alleles along a haploid genome with marginal probability of archaic ancestry > 0.50. We merged the inferred archaic haplotypes (Neanderthal haplotypes inferred across all non-Africans, Denisovan haplotypes inferred across all Oceanians). We reconstructed 2235 Neanderthal contigs that cover a total length of 673 Mb and 967 Denisova contigs with a total length of 257 Mb.

Genomic regions with elevated archaic ancestry

We screened for non-overlapping 100 Kb windows with elevated proportions of archaic ancestry as estimated by $la^{(a)}(w) = \frac{\sum_{s \in S(w)} \sum_{i=1}^I \gamma_{i,s}^{(a)}}{I|\{j \in S(w)\}|}$. Here I is the number of haploid genomes, $S(w)$ refers to the set of SNPs that belong to window w , $a \in \{n, d\}$ refers to either Neanderthal or Denisovan ancestries, and $\gamma_{i,s}^{(a)}$ refers to the marginal probability of archaic ancestry a at SNP s in individual i . We selected the windows with this statistic exceeding 0.30 and merged consecutive windows.

We identified a number of windows with elevated proportions of Neanderthal ancestry – 88, 27, 37, 116, 2 and 11 in American, Central Asian, East Asian, Oceanian, South Asian and West Eurasian populations respectively. Further, we identified 48 windows with elevated proportions of Denisovan ancestry in Oceanians (Table S4). Our scan recovered previously identified loci such as BNC2 in West Eurasians [S1; 17] as well as POU2F3 [S1]/TMEM136 [S17].

GO analysis

We tested whether specific sets of genes have significantly elevated frequencies of archaic ancestry. To do this, we classified CCDS genes as having high archaic ancestry if the gene ranked in the top 5% of genes ranked according to the average of the marginal probability of archaic ancestry across all SNPs within the gene and all individuals in the population. For Neanderthal ancestry in mainland Eurasians, we used the method from [S1] as it has greater power for populations with a single dominant archaic ancestry. For Neanderthal and Denisovan ancestry in Oceanians, we used the modified method proposed here. We then tested for an enrichment of Gene Ontology categories [S18] using the hypergeometric test implemented in FUNC [S19]. We report categories that are significant at the 0.05 level after multiple testing correction using 1000 permutations.

Analysis of genomic regions deficient in archaic ancestry

We searched for large regions that are deficient in Neanderthal and Denisovan ancestry in the different populations in SGDP, restricting our analysis to the Oceanian population (Australians, Papuans and Bougainville Islanders) in the case of Denisovan ancestry.

As described previously [S1], to assess the existence of regions deficient in archaic ancestry in a robust manner, we measured the fraction of archaic ancestry $ta_t^{(a)}(w)$ that exceeds a threshold t for archaic ancestry $a, a \in \{n, d\}$, averaged across all SNPs and individuals within window w :

$$ta_t^{(a)}(w) = \frac{\sum_{i=1}^I \sum_{s=1}^S \mathbf{1}\{\gamma_{i,s}^{(a)} > t\}}{I|\{s \in w\}|} \quad (2)$$

Here $t \in [0, 1]$ is a threshold. We chose $t = 0.25$ to reduce our false negative rate and chose to examine large windows ($w = 10$ Mb) that overlap each other by 1 Mb. We excluded all windows that overlap (over any part of their length) the centromeres or the telomeres. We further restricted our analysis to windows in which the number of SNPs that pass filters is at least 1000 and over which the genetic length ≥ 2 cM. We declared a window as a desert if $ta_t^{(a)}(w) < \frac{1}{1000}$ and merged overlapping deserts.

We identified a number of regions that are deserts for archaic ancestries in different populations of the SGDP. Of particular interest are regions that are deserts for both Neanderthal and Denisovan ancestries across all populations. We identified four windows longer than 10 Mb (1 : 99 – 112, 3 : 78 – 90, 7 : 108 – 128, and 13 : 49 – 61 Mb) that are deserts for both Neanderthal and Denisovan ancestries across all populations. The locus on chromosome 7 is particularly interesting as it contains the FOXP2 gene [S17]. This observation is interesting because previous attempts that identified deserts of Neanderthal ancestry [S17; 1] could not rule out the possibility that these deserts were the result of demographic events [S1]. The observation of deserts that are shared across distinct introgression events might suggest that these regions are resistant to introgression because of their importance for the modern human phenotype and represent selection against the introgressing alleles. To test the null hypothesis that the Neanderthal and Denisovan deserts are independently located along the genome, for each chromosome, we randomly placed the Neanderthal deserts (avoiding centromeres and telomeres since the original deserts were chosen to be non-overlapping with these features) and then counted the length of intersection of these deserts to the Denisovan desert. The P-value we report is the proportion of random datasets for which the overlap length is longer than that observed in data. We obtain a permutation p-value 0.67. We also observe two shared deserts larger than 10 Mb on chromosome X ($X : 62 – 78$, $X : 109 – 143$ Mb).

Correlation of archaic ancestry with B-statistics

To interrogate the effects of selection against introgressing archaic alleles, we analyzed the proportion of archaic ancestry in a genomic region as a function of the B-statistic, a measure of background selection [S20].

B-statistics were lifted over to hg19 coordinates. We then annotated each of the SNPs that we analyzed with the B-statistic of the genomic region in which the SNP falls. In our first analysis, we partitioned SNPs into quintiles based on their B-statistic annotation. At each SNP, we considered several estimates of the archaic ancestry : $la^{(a)}$ which computes the average over the marginal probability of archaic ancestry assigned to each individual haplotype, $ta_{0.9}^{(a)}$ which computes the average fraction of alleles across individuals that attain a marginal probability of ≥ 0.90 and $ta_{0.25}^{(a)}$ that computes the analogous statistic for a threshold of 0.25. Under a model where the archaic alleles are not under purifying selection, the power to detect archaic ancestry increases with decreasing B-statistic [S1] so that we expect the summaries of archaic ancestry to increase with decreasing B. On the other hand, under a model where the archaic alleles are subject to purifying selection, these statistics are expected to decrease with decreasing B.

We estimated Spearman’s correlation coefficient ρ between Neanderthal ancestry and B-statistic in West Eurasians, East Asians and Oceanians (Table S6). We performed a block jackknife in 10 Mb windows to estimate the standard error of ρ . We see a statistically significant correlation between B-statistic and different summaries of the Neanderthal ancestry. The significance is strongest for the *la* statistic on the autosomes. While the *ta* statistics are not always significant, this trend is expected given the reduction in power to detect archaic ancestry with increasing value of B [S1] and that increasing the threshold is bound to exacerbate the difference in power across B quintiles. We also see an analogous, though weaker, trend on the X as would be expected given the reduced number of observations on the X.

Next, we estimated ρ for the Denisovan ancestry in Oceanians and observed an analogous positive correlation of *la* with B consistent with the effect of purifying selection on Denisovan introgressed alleles (Table S6).

Association of Denisovan ancestry with tissue-specific expression

We analyzed the Illumina BodyMap 2.0 data for genes that are highly expressed in each of 16 tissues. We used the definition of tissue-expressed genes in [S1] as genes that are significantly highly expressed in a given tissue than in any of the other tissues using the DESeq package [S21]. We defined a gene as being depleted in Denisovan (Neanderthal) ancestry when all sites across all Oceanian (Melanesian, Australian and Bougainville) individuals in the gene are assigned a marginal probability ≤ 0.10 . We tested whether there is a statistically significant enrichment of tissue-expressed genes in genes with depleted Denisovan (Neanderthal) ancestry. We also tested for enrichment of tissue-expressed genes in genes depleted for Neanderthal ancestry in mainland Eurasians defined as a gene that is depleted in each of West Eurasian, East Asian, South Asian, American and Central Asian maps.

As a check for whether testes-specific genes might be depleted in archaic ancestry due to differences in the strength of purifying selection, we compared the B-statistics across testes-expressed genes to other tissue-expressed genes. For each gene, we computed an average B-statistic [S20]. Testes-expressed genes had a slightly reduced B-statistic on average compared to other tissue-expressed genes (0.673 ± 0.007 vs 0.684 ± 0.004) but the reduction is not statistically significant (Mann-Whitney one-sided test P-value = 0.07). Other tissue-expressed gene sets such as liver, heart and skeletal muscle have lower average B-statistics than testes but do not show a statistically significant depletion in archaic ancestry. We further investigate the influence of the B-statistic by performing a logistic regression of the depletion status of each tissue-expressed gene using as covariates the specific tissue in which it is expressed as well as the B-statistic. Table S7 shows that only testes-expressed genes are enriched in regions of low archaic ancestry.

It is plausible that the B-statistic is not strongly correlated with selective constraint, particularly in testes-expressed genes. To further investigate this possibility, we estimated the local heterozygosity at each gene. To reduce the potential for interaction between the local heterozygosity and the accuracy of our method for archaic ancestry inference, we estimated the local heterozygosity for each gene is calculated across 76 African chromosomes in the SGDP, restricting to sites which pass filter level ≥ 1 , and to sites where at least half the samples have a valid genotyping call. Samples from panel A were excluded as the error rate is known to be higher. We then repeated the analysis carried out using B-statistics but now replacing B-statistics with local heterozygosity. Table S7 shows that, under this model, testes-expressed genes remain the only set of genes that are enriched in regions of low archaic ancestry.

Supplemental References

- S1. S. Sankararaman, S. Mallick, M. Danneman, K. Prüfer, J. Kelso, S. Pääbo, N. Patterson, and D. Reich. The landscape of Neandertal ancestry in present-day humans. *Nature*, 2014.
- S2. Qiaomei Fu, Heng Li, Priya Moorjani, Flora Jay, Sergey M Slepchenko, Aleksei A Bondarev, Philip LF Johnson, Ayinuer Aximu-Petri, Kay Prüfer, Cesare de Filippo, et al. Genome sequence of a 45,000-year-old modern human from western siberia. *Nature*, 514(7523):445–449, 2014.
- S3. S. Sankararaman, N. Patterson, H. Li, S. Pääbo, and D. Reich. The date of interbreeding between Neandertals and modern humans. *PLoS Genet.*, 8(10):e1002947, 2012.
- S4. G. Coop, X. Wen, C. Ober, J. K. Pritchard, and M. Przeworski. High-resolution mapping of crossovers reveals extensive variation in fine-scale recombination patterns among humans. *Science*, 319:1395–1398, Mar 2008.
- S5. Hans R Kunsch. The jackknife and the bootstrap for general stationary observations. *The Annals of Statistics*, 17(3):1217–1241, 1989.
- S6. K. Prüfer, F. Racimo, N. Patterson, Flora. Jay, S. Sankararaman, and S. Sawyer. The complete genome sequence of a neandertal from the altai mountains. *submitted*, 2013.
- S7. Matthias Meyer, Martin Kircher, Marie-Theres Gansauge, Heng Li, Fernando Racimo, Swapan Mallick, Joshua G. Schraiber, Flora Jay, Kay Prüfer, Cesare de Filippo, Peter H. Sudmant, Can Alkan, Qiaomei Fu, Ron Do, Nadin Rohland, Arti Tandon, Michael Siebauer, Richard E. Green, Katarzyna Bryc, Adrian W. Briggs, Udo Stenzel, Jesse Dabney, Jay Shendure, Jacob Kitzman, Michael F. Hammer, Michael V. Shunkov, Anatoli P. Derevianko, Nick Patterson, Aida M. Andrés, Evan E. Eichler, Montgomery Slatkin, David Reich, Janet Kelso, and Svante Pääbo. A high-coverage genome sequence from an archaic denisovan individual. *Science*, 2012.
- S8. Swapan Mallick, Heng Li Li, Mark Lipson, Iain Mathieson, Melissa Gymrek, Fernando Racimo, Mengyao Zhao, and Niru Chennagiri. The landscape of human genome diversity. *in review*, 2015.
- S9. Simon Myers, Leonardo Bottolo, Colin Freeman, Gil McVean, and Peter Donnelly. A fine-scale map of recombination rates and hotspots across the human genome. *Science*, 310(5746):321–324, 2005.
- S10. Simon Gravel, Brenna M Henn, Ryan N Gutenkunst, Amit R Indap, Gabor T Marth, Andrew G Clark, Fuli Yu, Richard A Gibbs, Carlos D Bustamante, David L Altshuler, et al. Demographic history and rare allele sharing among human populations. *Proceedings of the National Academy of Sciences*, 108(29):11983–11988, 2011.
- S11. F Busing, E Meijer, and R Leeden. Delete-m jackknife for unequal m. *Statistics and Computing*, 9:3–8, 1999.
- S12. H. Li. Aligning sequence reads, clone sequences and assembly contigs with BWA-MEM. *ArXiv e-prints*, March 2013.
- S13. Mark A DePristo, Eric Banks, Ryan Poplin, Kiran V Garimella, Jared R Maguire, Christopher Hartl, Anthony A Philippakis, Guillermo Del Angel, Manuel A Rivas, Matt Hanna, et al. A framework for variation discovery and genotyping using next-generation dna sequencing data. *Nature genetics*, 43(5):491–498, 2011.
- S14. Olivier Delaneau, Jonathan Marchini, and Jean-François Zagury. A linear complexity phasing method for thousands of genomes. *Nature methods*, 9(2):179–181, 2012.

- S15. J. D. Wall, M. A. Yang, F. Jay, S. K. Kim, E. Y. Durand, L. S. Stevison, C. Gignoux, A. Woerner, M. F. Hammer, and M. Slatkin. Higher Levels of Neanderthal Ancestry in East Asians Than in Europeans. *Genetics*, Feb 2013.
- S16. Emilia Huerta-Sánchez, Xin Jin, Zhuoma Bianba, Benjamin M Peter, Nicolas Vinckenbosch, Yu Liang, Xin Yi, Mingze He, Mehmet Somel, Peixiang Ni, et al. Altitude adaptation in tibetans caused by introgression of denisovan-like dna. *Nature*, 512(7513):194–197, 2014.
- S17. Benjamin Vernot and Joshua M Akey. Resurrecting surviving neandertal lineages from modern human genomes. *Science*, 343(6174):1017–1021, 2014.
- S18. M. Ashburner, C. A. Ball, J. A. Blake, D. Botstein, H. Butler, J. M. Cherry, A. P. Davis, K. Dolinski, S. S. Dwight, J. T. Eppig, M. A. Harris, D. P. Hill, L. Issel-Tarver, A. Kasarskis, S. Lewis, J. C. Matese, J. E. Richardson, M. Ringwald, G. M. Rubin, and G. Sherlock. Gene ontology: tool for the unification of biology. The Gene Ontology Consortium. *Nat. Genet.*, 25(1):25–29, May 2000.
- S19. K. Prufer, B. Muetzel, H. H. Do, G. Weiss, P. Khaitovich, E. Rahm, S. Paabo, M. Lachmann, and W. Enard. FUNC: a package for detecting significant associations between gene sets and ontological annotations. *BMC Bioinformatics*, 8:41, 2007.
- S20. Graham McVicker, David Gordon, Colleen Davis, and Phil Green. Widespread genomic signatures of natural selection in hominid evolution. *PLoS Genet*, 5(5):e1000471, 05 2009.
- S21. Simon Anders and Wolfgang Huber. Differential expression analysis for sequence count data. *Genome Biol*, 11(10):R106, 2010.